Inverse Problems, Design and Optimization Symposium
Rio de Janeiro, Brazil, 2004

AN INVERSE SOLUTION TO 3-D SOURCE LOCALIZATION OF EPILEPTIC FOCI USING AN INTEGRATED MULTIMODAL NEURO-IMAGING APPROACH

Malek Adjouadi, Natasa Mirkovic, Mercedes Cabrerizo, and Melvin Ayala
Center for advanced Technology and Education
Department of Electrical & Computer Engineering, Florida International University,
10555 W. Flagler Street, Miami FL 33174, Tel: (305) 348-3019,
Emails: adjouadi@fiu.edu, Natasa.mirkovic@fiu.edu, mercedes.cabrerizo@fiu.edu, Melvin.Ayala@fiu.edu

Abstract

This study proposes an inverse solution in estimating the 3-D localization of interictal spike activity in epileptogenic data. Sensory modalities for data analysis include electroencephalographs (EEG) superimposed on magnetic resonance imagery (MRI) in a pediatric population with extra-temporal lesional epileptic foci. In this integrated approach, software developments were based on a three-dimensional (3-D) programming platform driven by multimodal neuro-imaging software, namely the CURRY program. The inverse solution is supported by a simplex optimization method. To circumvent false local minima, iterations are repeated from several initial dipoles scattered in various locations. Values of the minima reached by these initial dipoles reveal localization accuracies of clinical relevance. This approach was adapted for analyzing scalp EEG data and reconstructing superimposed images in 10 children who underwent extensive pre-surgical evaluation for intractable partial seizures. The results of 3-D spike source localization were assessed in relationship to focal lesions evident on the patient's MRI scans.

1. INTRODUCTION

Epilepsy surgery is now being increasingly performed in children with medically refractory partial seizures. Seizures often arise from extra-temporal sites and are related to a malformed pathologic substrate that is more extensive than the lesion evident on MRI scans. Presurgical evaluation is therefore more difficult than in adults and relies heavily on EEG data including interictal spike discharges. The spikes recorded on the scalp can be processed using specialized software (such as CURRY) to define their source in 3-D that can then be superimposed on the patient's MRI scan to further facilitate surgical planning. A detailed overview of the different source reconstruction methods can be found (Ossenblok et al. 1999 and Baillet et al. 2001). While this technique has been used successfully in adults being evaluated mainly for temporal lobe epilepsy, its application has been limited in the pediatric population.

This study adapted the CURRY program and assessed the relationship of the 3-D spike sources to focal lesions evident on MRI scans. We selected this subgroup as it represents an initial step in determining the merit of this technique in the pre-surgical evaluation of children. Further studies comparing reconstructed spike sources with intracranial electrode recording are planned.

2. METHOD

2.1 Participants

Ten children with medically refractory partial seizures undergoing pre-surgical evaluation have been analyzed in this study. MRI scans revealed focal developmental lesions that were mainly extra-temporal in location. The relevant information for all patients is given in Table I.

2.2 Recording Apparatus

The EEG data was recorded using XLTEK Neuroworks Ver.3.0.5 (equipment manufactured by Excel Tech Ltd. Ontario, Canada). The standard international 10-20 system with 21 electrodes was used. Sampling frequency of 500Hz with 0.1-70 Hz bandpass filter settings and 22 bits A/D conversion were used to obtain the digital EEG recordings.

MRI images were created using the Signa Horizon LX 1.5 Tesla MRI scanner (manufactured by General Electric, Medical Systems, Wisconsin, USA). High resolution T1 weighted spoiled GRASS (Gradient Recalled Acquisition in the Steady State) images were obtained.

2.3 Data Analysis

To identify the location of the epileptic sources, a source localization program was developed using the NeuroScan software CURRY V.3.0. Input data in this study were EEG signals and MRI brain images of epileptic patients.

The first step in the localization procedure involved identifying the pertinent time intervals in the overall EEG recordings in which the interictal spikes occurred. The physicians performed this task by visual inspection of the recorded data. These portions of EEG data were of 2-4 s duration and during these intervals the source localization analysis was performed using the CURRY based program.

In the preprocessing step DC and high frequency components were removed from the data using a 0.1-100 Hz band-pass filter. Specifically, a third order

Butterworth filter was implemented. To extract the dominant EEG patterns, the Singular Value Decomposition (SVD) method was applied where the first three largest singular values were retained to account for the useful EEG epileptic signal information.

MRI brain scans were used to construct realistic subject dependant head models. The model derived was a Boundary Element Model (BEM) consisting of three compartments. The compartments used were skin, skull and brain tissue. These were obtained by segmentation of the MRI images and they were assigned the following conductivities: 0.33, 0.0042 and 0.33 S/m respectively.

MRI images were also used to determine locations of scalp electrodes. Since the EEG was recorded using standard 10-20 system, the electrode positions were computed automatically in CURRY. For each patient, the electrode locations were determined from the segmented skin obtained by MRI segmentation, which led to subject-dependant electrode placement.

The method applied for source localization was the Moving Dipole Solution, available in CURRY. The result obtained by implementing this method is the calculated location of the dipole in the form of a point $r_{qc} = (x_{qc}, y_{qc}, z_{qc})$ in Cartesian coordinates and the strength of the dipole moment. Also, for each patient the anticipated coordinates $r_{qa} = (x_{qa}, y_{qa}, z_{qa})$ of the nearest edge of the actual lesions and/or tubers in the MR images were identified by visual inspection. These abnormalities in the MRI were clinically assumed to be the true sources of the epileptic seizures.

The time interval during which the source localization was performed was a 200ms time range, which is a typical duration of an epileptic spike. The 200ms time range was defined around the center of the spike with a largest magnitude. Furthermore, it was divided into five 40ms intervals where the central interval corresponded to the peak of the spike as shown in Figure 1. A single dipole was fitted every 10 ms during each interval. For each interval dipole location closest to the nearest edge of the actual anticipated epileptic focus was chosen, leading to five points that describe the source trajectory during the epileptic spike. Such detailed analysis allows tracking the propagation of the epileptic activity throughout the brain, which offers insight into the brain dynamics and, and as a consequence, facilitates identification of the brain areas that are to be surgically removed.

Finally, the Euclidian distance was calculated between the point that represents the calculated dipole location, $r_{qc} = (x_{qc}, y_{qc}, z_{qc})$ and the anticipated point representing abnormality in the MRI, $r_{qa} = (x_{qa}, y_{qa}, z_{qa})$, defined by the nearest edge of the structural lesion. This distance was introduced as a means of representing the error of the localization procedure.

3. INTEGRATED 3-D LOCALIZATION SOLUTION

Details on the modeling of the EEG signals, the mathematics of SVD, Result confirmation through the discrete cosine transform (DCT), EEG spatio-temporal filtering, least squares and moving dipole method follow.

3.1. Modeling of EEG Signals

The propagation of EEG signals through the head is modeled using the principles of electromagnetism. EEG signals represent the electric waves and the head is modeled as a volume conductor. Maxwell's equations are used to describe the behavior of EEG signals. Specifically, the model is based on the quasi-static approximation of Maxwell's equations. It is reasonable in this study to make this simplifying assumption, since the frequency range of interest in the case of EEG signals is generally in the range of 0.1-100Hz (Baillet et al. 2001).

If the location and the strength of the source are known, and the goal is to calculate the surface potential generated by that source, the EEG modeling is often referred to as *forward modeling*. Forward model equations do not have an analytical form in the general case. However, if specific models of the electric source and volume conductor are assumed, analytical and numerical solutions can be derived.

If the head is modeled as the multilayered surface of *m* non-intersecting homogenous regions of constant isotropic conductivity, the electric potential on any of the *m* boundary surfaces between two neighboring head regions is given by equations (1) and (2), (Ermer et al. 2001, Tripp et al. 1983):

$$V(\mathbf{r}) = \frac{2\sigma_0}{\sigma_j^- + \sigma_j^+} V_0(\mathbf{r}) - \frac{1}{2\pi(\sigma_j^- + \sigma_j^+)} * \left\{ \sum_{i=1}^{m} (\sigma_i^- - \sigma_i^+) \int_{S_i} V(\mathbf{r}') \frac{\mathbf{r} - \mathbf{r}'}{|\mathbf{r} - \mathbf{r}'|^3} d\mathbf{S}_i \right\} \quad (1)$$

$$V_0(\mathbf{r}) = \frac{1}{4\pi\sigma_0} \int_G \mathbf{J}_\mathbf{p}(\mathbf{r}') \frac{(\mathbf{r} - \mathbf{r}')}{|\mathbf{r} - \mathbf{r}'|^3} d\mathbf{r}' \quad (2)$$

where $r = (x, y, z) \in S_j$ is the location from which it is desired to calculate the potential and **r'** the location of a source point. σ_0 is the conductivity of the point **r** where the potential is calculated, S_i, i = (1, 2, 3) is the surface between the neighboring regions of conductivity σ_i^- and σ_i^+. Integration is performed over the whole surface S_i and its vector element is presented by dS_i. There are two parts contributing to electric potential in equation (1). The first term depends on $V_0(r)$ and is generated by the source currents characterized by the current density distribution J(r') within the region *G*. Potential $V_0(r)$ is calculated following equation (2),

which defines the potential in the case of an infinite homogenous volume conductor of conductivity σ_0. The second term in equation (1) is due to the existence of the boundary surfaces S_i that are behaving as the secondary sources of the electric field.

The most often used model to represent the source of brain activity is the current dipole. It is an extension of the electric dipole and it consists of the current source and sink that inject and remove the same amount of current *I* (Shindo et al, 1998; Merlet and Gotman, 1999; Scherg and Ebersole, 1993). The distance between the source and the sink is **d** and the position of the dipole $\mathbf{r_q}$ is defined at d/2. The dipole is characterized by its electric moment defined as $\mathbf{q} = I \cdot \mathbf{d}$. In this specific case, where the source is presented by a current dipole equation (2) can be simplified as:

$$V_0(\mathbf{r}) = \frac{1}{4\pi\sigma_0} \frac{\mathbf{q} \cdot (\mathbf{r} - \mathbf{r}_q)}{\left|\mathbf{r} - \mathbf{r}_q\right|^3} \qquad (3)$$

Equation (1) defines the potential at any location **r** on the surfaces between different tissue regions. However, the potentials of interest are only those that can be measured at the locations of the electrodes $m(\mathbf{r}_i)$ and they can be derived from (1) and (3) in the following form (Ermer et al. 2001):

$$\begin{bmatrix} m(\mathbf{r}_1) \\ \dots \\ m(\mathbf{r}_n) \end{bmatrix} = \begin{bmatrix} l(\mathbf{r_1}, \mathbf{r}_q) \\ \dots \\ l(\mathbf{r_n}, \mathbf{r}_q) \end{bmatrix} \mathbf{Q} \qquad (4)$$

where $m(\mathbf{r}_i)$, *i*=(1,2, …n) are EEG potentials measured by *n* electrodes at locations $\mathbf{r_i}$ generated by a dipole with location $\mathbf{r_q} = (x_q, y_q, z_q)$ and moment $\mathbf{Q} = (q_x, q_y, q_z)^T$. Compact matrix representation of equation (4) is given by:

$$\mathbf{M} = \mathbf{LQ} \qquad (5)$$

where **L** is the lead-field matrix, which projects the source to the *n* scalp recording sites.

Generally, no matter which of the head models is implemented, by electromagnetic superposition the electric potential is linear in dipole moment (Baillet et al. 2001 and Ermer et al. 2001), which leads to a simplified representation of the forward model given by (5), as the inner product of the lead-field and the dipole moment. The equations for calculating lead-field matrix depend on the head model used. They range from very simple relations for spherical head models to very complicated ones for realistic head shapes such as BEM model. Detailed description of different lead-field matrix calculation can be found in (Mosher et al. 1999).

Source reconstruction determines the 3-D location and strength of the source from the recorded EEG data. This is often referred to as the *inverse problem*. The main difficulty with solving the inverse problem is that it does not have a unique solution, since both **L** that represents location and **Q** representing source strength are unknown. However, the equation can still be solved iteratively by using the forward model and with the introduction of additional constraints for the solution. This solution framework is explained in the following sections.

3. 2. SVD and EEG Spatio-Temporal Filtering

Recorded EEG signals represent a composition of underlying epileptic activity along with different artifact signals such as eye blinks, EKG, EMG, and interference introduced by the measurement itself. In order to achieve accurate localization results, the first step in the analysis is to extract the dominant epileptic activity from the overall EEG data (Mosher et al. 1998). A mathematical approach that allows for such an outcome is the Singular Value Decomposition method SVD (Gençer et al. 1998, Chen 1998, Moon et al 2000). This transform decomposes a given matrix **M** into three different matrices as follows:

$$\mathbf{M} = \mathbf{U\Sigma V^T} \qquad (6)$$

with $\mathbf{\Sigma} = diag(\sigma_i)$. Matrices **U** and **V** are orthogonal and $\mathbf{\Sigma} = diag(\sigma_i)$ is a diagonal matrix containing singular values in the descending order as its elements. This relation can also be represented as

$\mathbf{M} = \sum_{i=1}^{n} \sigma_i^{1/2} u_i v_i^T$, where u_i are the vectors of **U**, v_i vectors of **V** and *n* is the number of rows of matrix **M**, which is equal to a number of electrodes used for recording.

Each singular value is associated with an orthogonal pattern contained in the data matrix **M**. Larger singular values correspond to higher pattern correlation with the original data. Therefore, SVD allows the extraction of dominant patterns from the recorded EEG data by keeping the largest singular values and setting to zero those with small values assuming that they correspond to noise and other artifacts. Application of SVD in this fashion has the effect of spatio-temporal filtering, since EEG data is stored in a matrix, whose rows represent electrodes and carry spatial information, and whose columns represent time samples containing temporal information. However, it is not always true to assume that each SVD pattern is generated by a single source, since SVD patterns are mathematically orthogonal, which is not the case with actual biological EEG sources.

3.3 Confirmation of Results based on the Discrete Cosine Transform

Although the SVD method is sound in its application, it makes practical sense to confirm such results through an automated approach to interictal spike detection based on the DCT, in order to augment and confirm the results obtained through the SVD approach. This particular design step focuses on the use of orthogonal operators based on unique signal decompositions in order to detect interictal spikes that characterize epileptic seizures in EEG data. The merits here are in establishing mathematical derivations that provide quantitative measures through the designed operators, and characterize and locate the event of an interictal spike conform to the results of the SVD and prior to estimating the 3-D location using the inverse solution of Least Squares and Moving Dipole Method.

Given the digitized input EEG signal, $f(t)$, the DCT transform defined by C_N^r is given by the convolution ($*$) of ω_N^r with $f(t)$ as:

$$C_N^r = c_N^r * f(t) \tag{7}$$

where the DCT transform kernel c_N^r used in equation (7) is as defined below:

$$c_N^r = \sqrt{\frac{2}{N}} \sum_{x=0}^{N-1} \cos \frac{(2x+1)r\pi}{2N} \tag{8}$$

In equation 8, coordinate x identifies the kernel element in a given row r. For mathematical purposes, the first row is identified by $r = 0$. Therefore, the cosine operator of 1st order (r =1) and length 2 (N=2), is functionally equal to the 1st derivative, d^1; and the cosine operator of 2nd order and length 4, is functionally equivalent to the 2nd derivative, d^2.

After DCT transformations are performed, and in order to enhance identification of the sharp and steep transitions of potential spikes, the DCT results at different scales (resolutions used are N=4, 8, and 16) are added together to detect all potential transitions under different scaling (as revealed through higher amplitudes), which is expressed in the corresponding graphs as:

$$C^r = C_4^r + C_8^r + C_{16}^r \quad \text{for r} = 1,2 \tag{9}$$

Since the interictal spike must exhibit high degrees of sharpness in narrow and wider intervals, the resulting measures of sharpness/steepness in these intervals can be extracted through the functional equivalence of performing first and second order derivatives on the results obtained in the previous step. This is achieved with a point-by-point multiplication between the equivalent to the first and second order cosine operators (equivalent to mathematical first and second derivatives), given by C_2^1 and C_2^4, and the addition of the cosine operators of different lengths *N*, given by $C_4^r + C_8^r + C_{16}^r$ (r =1, 2) as performed earlier. In other words the following operations are performed in this step to emphasize that part of the signal that meets sustained steep slopes and sharp peak, which characterize a spike:

$$C1 = C_2^r . C^r = C_2^r \cdot [C_4^r + C_8^r + C_{16}^r], r = 1 \tag{10}$$

$$C2 = C_{2+r}^r . C^r = C_{2+r}^r \cdot [C_4^r + C_8^r + C_{16}^r], r = 2$$

Note as shown in the illustrative example of Figure 2, how in the results potential spikes are predominant with respect to the background. Dynamic thresholding is assumed in the next two graphs labeled as CT1 and CT2 as thresholded version of C1 and C2 from the previous step. In order to extract that part of the signal deemed important from background activity, the threshold (T) was computed as one standard deviation above the mean of all the peaks found in 3s windows. The next and final two graphs denoted by CT1* and CT2* contain only those components of the signals in CT1 and CT2 that satisfy all the established criteria delineated by the two peaks in CT1* which are indicative of the steepness of the rising and falling slopes of the spike, and the one prominent peak in CT2* which accurately depicts the spike's peak location, and whose amplitude is related to the sharpness of the spike.

3.4 Least Squares and Moving Dipole Method

As previously explained, EEG source localization is a problem which does not have a unique inverse solution (Baillet et al. 2001, Gençer et al. 1998, Mosher et al. 1995). The Least-Squares solution (LS) introduces additional constraints so that a single solution may be determined. It is an iterative optimization procedure that minimizes the squared difference between the measured potentials, $\mathbf{M}_{\mathbf{meas}}$ and potentials generated by the estimated dipole, $\mathbf{M}$ can be determined from equation (11) as:

$$J_{LS} = \left\| \mathbf{M}_{\mathbf{meas}} - \mathbf{M} \right\| = \left\| \mathbf{M}_{\mathbf{meas}} - \mathbf{LQ} \right\|^2 \tag{11}$$

where operator $\| \ \|$ represents Frobenius norm.

The LS algorithm starts with an initial estimate for the dipole location and calculates the lead field matrix $\mathbf{L} = \mathbf{L}(\mathbf{r}_q, \mathbf{r})$ for that dipole location. Dipole strength $\mathbf{Q}$ that minimizes the cost function J_{LS} is given by:

$$\mathbf{Q} = \mathbf{L}^{+}\mathbf{M}_{\mathbf{meas}} = \sum_{i-1}^{n} \frac{1}{\sigma_i} (u_i^T \mathbf{M}_{\mathbf{meas}}) v_i \tag{12}$$

where $\mathbf{L}^{+}$ represents the pseudo-inverse of $\mathbf{L}$ which is obtained from SVD transformation as:

$$\mathbf{L}^{+} = \mathbf{V}\boldsymbol{\Sigma}^{+}\mathbf{U}^{\mathbf{T}} = \sum_{i=1}^{r} \frac{1}{\sigma_i} v_i \, u_i^T \qquad (13)$$

Next, the squared difference between the calculated and measured data is calculated and the new dipole location is updated in such a way that it minimizes the previously calculated error. These steps are repeated until dipole location $r_{qc} = (x_{qc}, y_{qc}, z_{qc})$ is determined for which the error is less then some previously specified threshold.

The minimization technique should converge quickly but, at the same time, avoids local minima. The search for the minimum error is usually performed using the simplex optimization method. To avoid false local minima, iterations are usually repeated from several initial dipoles scattered in various locations. Values of the minima reached by these initial dipoles are compared and the smallest one is selected as the true minimum.

The procedure described is done for a single time sample of the recorded EEG and it yields a single dipole location. If it is performed over a time period that is for the number of consecutive EEG time samples, a dipole location is obtained for each of these samples. If this result is sequentially presented, the actual propagation of the source can be obtained. This type of solution represents the Moving Dipole Solution.

4. RESULTS

The results obtained for all patients are given in Table II in the form of the distance between computed 3-D dipole location $r_{qc} = (x_{qc}, y_{qc}, z_{qc})$, and the nearest edge of the actual anticipated epileptic focus $r_{qa} = (x_{qa}, y_{qa}, z_{qa})$ as provided by board certified radiologists reviewing MRI data.

The source localization analysis was performed every 10ms during the 200ms interval in which the spike occurred. This interval analysis allowed us to track the propagation of the source of epileptic activity from the onset of the spike to the generation of the slow wave representing the ending of the spike. Since the whole spike duration is divided into five 40ms intervals, the analysis yields four source locations per interval. Additionally, for each source location the distance from the lesion was calculated and for each interval the best among these four solutions, meaning the source with the minimum distance from the lesion, is presented in Table II. In Figure 3 the results obtained for each interval for all of the patients are illustrated. The middle interval, Interval 3 yielded best results for 6 out of 10 patients. The mean value and the variance were also calculated for each interval. The values obtained are illustrated in Figures 4 and 5 respectively. Interval 3 had the smallest mean value and variance making it to be the interval of choice for source localization of the epileptic foci. The average error calculated for the best solution for all of the 10 patients was 9 mm.

For visual appreciation, illustrative examples of the complete results of the integrated EEG-MRI approach for patients 3 and 5 are provided in Figures 6 and 7.
It is important to note that 6 of these 10 patients underwent successful surgical interventions. The other four patients had also successful surgical interventions but prior to this study, but our results did confirm the clinical findings.

5. CONCLUSION

This preliminary study evaluated an integrated approach to the 3-D localization of epileptic spikes. The full process integrated the Singular Value Decomposition (SVD) method in the analysis of EEG data, using the multimodal neuro-imaging software named CURRY to optimize the accuracy of the 3-D localization results. The reconstructed 3-D sources correlated well with MRI lesions and complemented visual analyses of scalp EEG data. The superimposed images facilitated placement of intracranial electrodes for further defining the epileptogenic region and led to successful surgical interventions.

The results of the interval analysis showed that the calculated 3-D sources were closest to the lesions corresponding to the peak of the spike. This finding may be because the peak by virtue of its highest electrical field values, best distinguishes the epileptic spike from the background activity. Nonetheless, interval analyses and moving dipole models provide a powerful tool for studying spikes propagation and have important pathophysiological implications.

The results are most encouraging, considering that the 3-D sources were computed using only the standard 10-20 system electrode placement. The use of closely spaced electrode array and averaging of multiple spikes in each subject will likely enhance the precision of 3-D localization and add to the merit of this technique. The results were useful in surgical planning in six children that underwent successful resections. This integrated technique may be further compared to intracranial EEG data as our next research step.

ACKNOWLEDGMENTS

The authors are grateful for the support provided by the National Science Foundation Grants EIA-9906600 and HRD- 0317692, and the Office of Naval Research Grant N00014-99-1-0952, as well as the NSF Graduate Research Fellowships for Ms. Mercedes Cabrerizo. The support of Miami Children's Hospital is greatly appreciated.

REFERENCES

Baillet S., Mosher J.C. and Leahy R.M. Electromagnetic Brain Mapping, IEEE Sig. Proc.Mag., November 2001, Vol. 18, No. 6: 14 –30

Chen J.J., Yeh J. and Tsa J., Initial Estimation Methods For Dipole Modeling In Localization Of Epileptogenic Focus, Med. Eng. & Phys. 20 ,1998: 11-20

Ebersole J.S., Noninvasive Localization of Epileptogenic Foci by EEG Source Modeling, Epilepsia, 41(Suppl. 3) , 2000: 24-33

Ermer J. J., Mosher J.C., Leahy R. M. and Baillet S., Rapidly recomputable EEG forward models for realistic head shapes, Phys. Med. and Biol. Mag. 46, 2001: 1265-1281

Koh S., Jayakar P., Resnick T., Alvarez L., Liit R.E. and Duchowny M., The localizing value of ictal SPECT in children with tuberous sclerosis complex and refractory partial epilepsy, Epileptic Disorders Vol 1, No. 1, March 1999:41:46

Nevzat G.G. and Williamson S.J., Differential Characterization of Neuronal Sources with the Bimodal Truncated SVD Pseudo-Inverse for EEG and MEG Measurements, IEEE Trans. Biomed. Eng. Vol. 45, No. 7, July 1998: 827-838

Merlet I. and Gotman J., "Reliability of Dipole Models of Epileptic Spikes", Clin. Neurophysiol., Vol. 110 (6), 1999: 1013-28

Moon T.K. and Stirling W.C., Mathematical Method and Algorithms for Signal Processing, Prentice Hall, 2000: 369-395

Multi-Modal Neuro-Imaging, User Guide CURRY, for CURRY Version 3.0, First Edition, February 1998.

Mosher J.C.,. Leahy R.M and Lewis P. S., Matrix Kernels For MEG and EEG Source Localization and Imaging, Acoustics, Speech, and Signal Processing, 1995. ICASSP-95., Volume: 5, 1995: 2943-2946

Mosher J.C., Leahy R.M. and Lewis P.S., EEG and MEG: Forward Solutions for Inverse Methods, IEEE Trans. Biomed. Eng. Vol. 46, No. 3, March 1999: 245-258

Mosher J.C. and Leahy R.M., Recursive MUSIC: A framework for EEG and MEG Source Localization, IEEE Trans. Biomed. Eng., Vol. 45, No. 11, November 1998: 1342-1354

Nenonen J., Purcell C.J., Horacek B.M., Stroink G. and Katila T., Magnetocardiographic functional localization using a current dipole in a realistic torso, IEEE Trans. Biomed. Eng., Vol 38, No. 7, July 1991: 658-664

Ossenblok P., Fuchs M., Velis N.D., Veltman E., Pijin J.P. and Lopes da Silva F. H., IEEE Eng. Med. Biol. Mag. May/Jun 1999: 67-77

Sherg M. and Ebersole J.S., "Models of Brain Sources", Brain Topogr., Vol. 5 (4), 1993: 419-423

Shindo K., Ikeda A., Musha T., Terada K., Fukuyama H., Taki W., Kimura J., and Shibasaki H., "Clinical Usefulness of the Dipole Tracing Method for Localizing Interictal Spikes in Partial Epilepsy", Epilepsia, Vol. 39 (4), 1998: 371-379

Tripp J., Physical concepts and mathematical models, Biomagnetism: An interdisciplinaty approach, Williamson S.J., Romani G.L., Kaufman L. and Modena I., Eds. New York: Plenum, 1983: 101-139

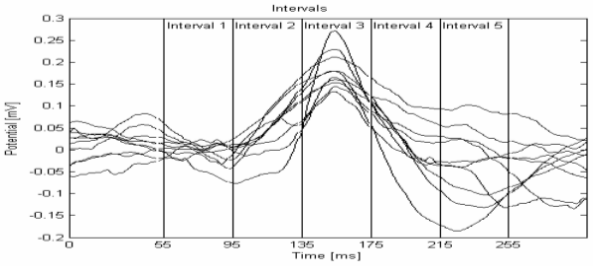

Figure 1: Spike intervals definition using 10 overlaid spikes

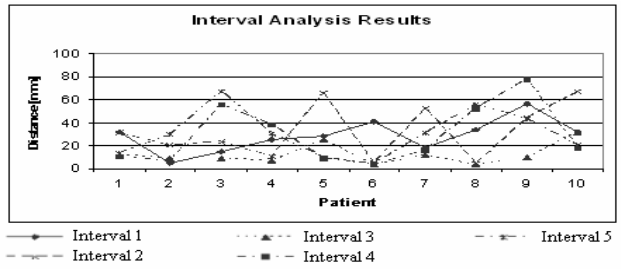

Figure 3: Spike interval results

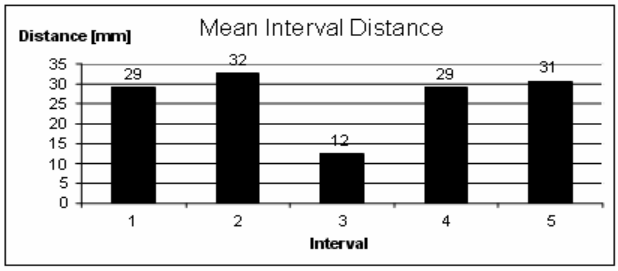

Figure 4: Mean of the interval distance

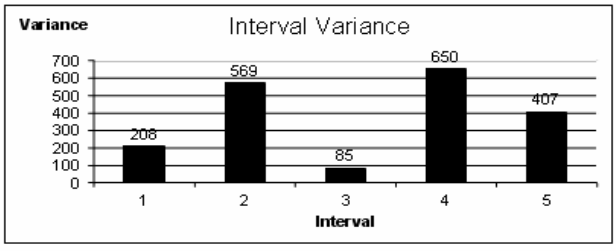

Figure 5: Variance of the interval distance

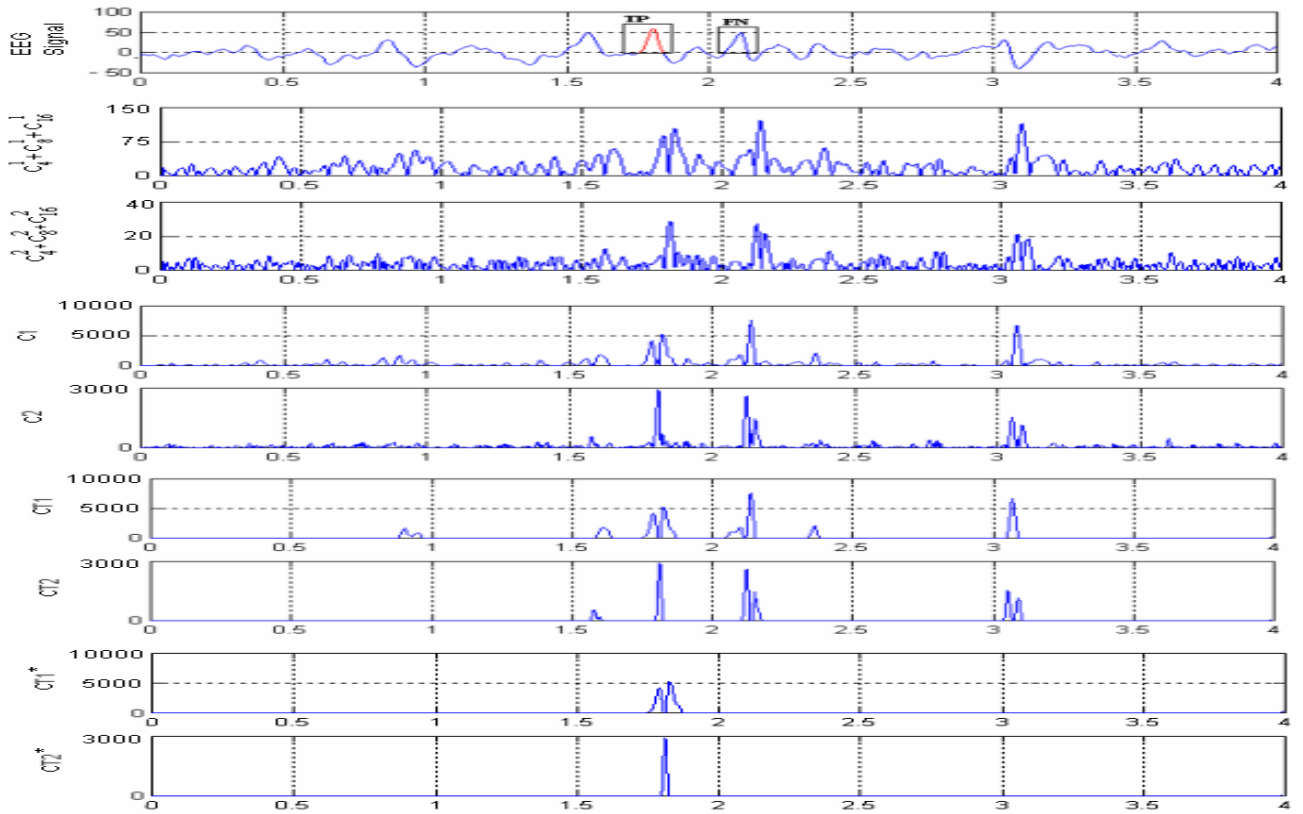

Figure 2: Spike detection using DCT operators showing a true positive (TP) and a false negative (FN)

Table 1: Patients used in the study and their respective diagnosis (Pat: Patient, RF: right frontal, LT: left temporal, LA: left anterior, LTO: left temporal occipital, LCP: left central parietal, RFT: right frontal temporal, LPQ: left posterior quadrant, RPT: right posterior temporal, RPQ: right posterior quadrant, LFC: left frontal central; age in d, m, a: days, months, years)

Diagnosis/ Syndrome	Pat.	Age	Interic. Spikes	Ictal Spikes	Seizure Type	MRI
Tuberous Sclerosis	**1**	13 m	RF	RF	Partial complex seizure with secondary generalization	Right frontal cortical dysplasia
	2	15d	LPQ	LPQ	Neonatal partial	Left temporal occipital junction tuber
	3	8a	RF	RF	Partial complex	Bifrontal tubers
Partial Epilepsy	**4**	17 a	RFT	RF	Simple partial	Right anterior and frontal cortical thickening
	5	10 a	RPT	RPQ	Partial complex	Right posterior quadrant lesion
	6	11 a	LA	LFC	Simple partial	Left frontal cortical dysplasia
	7	13 a	LT	N/A	Simple partial	Left temporal lesion
	8	4a	LCP	LCP	Partial complex	Left central lesion
	9	2a	LT	LTO	Simple partial	Left temporal and occipital lesion
	10	15 a	LT	LT	Partial complex	Left temporal cortical dysplasia

Table 2: Source localization error obtained for each patient (Pat.: patient, Int: Interval)

Pat.	Minimum Distance (mm)				
	Int. 1	Int. 2	Int. 3	Int. 4	Int. 5
1	32	31	12	11	14
2	5	20	9	7	30
3	26	11	7	38	30
4	15	24	9	56	67
5	29	66	26	9	10
6	41	5	3	4	4
7	19	52	12	16	31
8	34	5	3	53	56
9	57	44	10	78	43
10	32	67	32	18	21

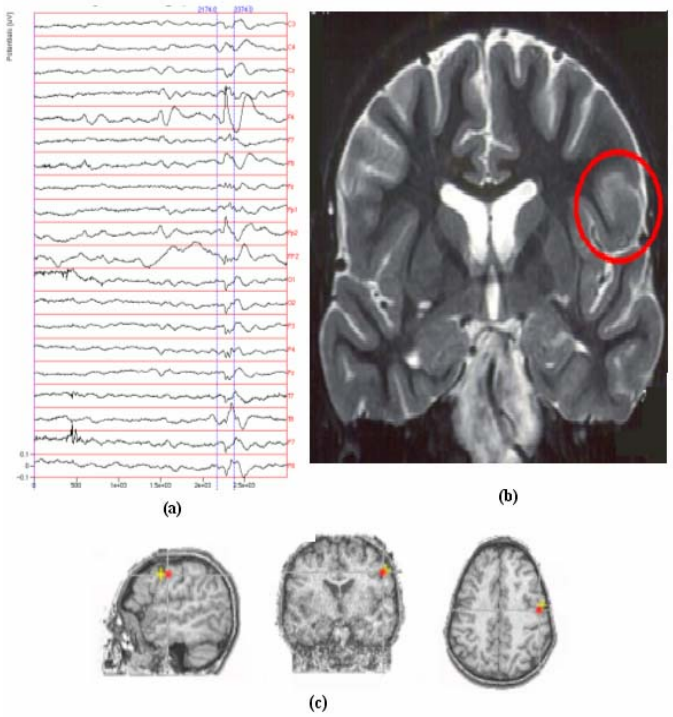

Figure 6: Results from the integrated EEG-MRI approach for the case of Patient 3: (a) EEG signals with interictal spikes extracted, (b) Lesion, (c) MRI representation of localization results
+Result from CURRY •Result from MRI

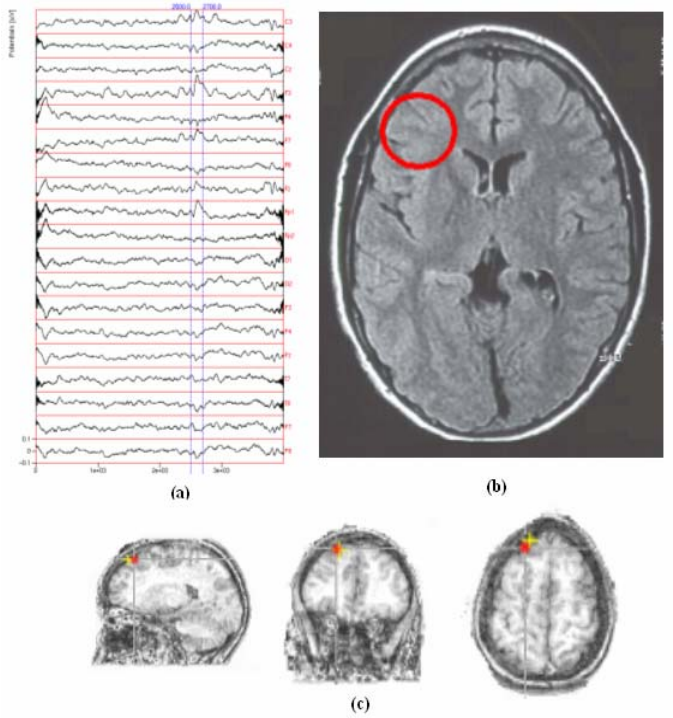

Figure 7: Results from the integrated EEG-MRI approach for the case of Patient 6: (a) EEG signals with interictal spikes extracted, (b) Lesion, (c) MRI representation of localization results:
+Result from CURRY •Result from MRI